El Cezeri
Journal of Science and Engineering
ISSN: 2148-3736

Research Article

# Dynamic Performance Analysis of D-STATCOMs for Mitigating Charging Station Impacts in Photovoltaic Distribution Systems Using Enhanced Hunter–Prey Optimization

**Pappu Soundarya Lahari[1a], Varaprasad Janamala[2b]**
[1]Electrical and Electronics Engineering Department, Christ University, Kengeri campus, Bangalore, India-560074
[2]Electrical and Electronics Engineering Department, Christ University, Kengeri campus, Bangalore, India-560074

pappusoundarya.lahari@res.christuniversity.in

DOI : 10.31202/ecjse.1809228
Received: 23.10.2025 Accepted: 08.04.2026
**How to cite this article:**
Lahari P.S., Janamala V., " Dynamic Performance Analysis of D-STATCOMs for Mitigating Charging Station Impacts in Photovoltaic Distribution Systems Using Enhanced Hunter–Prey Optimization ", El-Cezeri Journal of Science and Engineering, Vol: 13, Iss: 2, (2026), pp.(271-285).
ORCID: [a]0000-0003-0873-241X, [b]0000-0001-9716-5458.

**Abstract** This study investigates the dynamic operational performance and optimal allocation of Distribution Static Compensators (D-STATCOMs) in PV–EV integrated distribution systems to mitigate the impacts of voltage fluctuations, increased power losses, and reactive power imbalances. An Enhanced Hunter–Prey Optimization (EHPO) algorithm is proposed in the study, incorporating chaotic initialization, adaptive parameter control, and Cauchy's mutation exploration strategy to improve global search capability and convergence reliability. The proposed method is validated on the IEEE 33, 69, and 118- bus distribution test systems under varying PV generation and EV charging demand scenarios. Results show that the EHPO-based D-STATCOM placement significantly reduces active power losses and enhances voltage stability. The findings highlight the effectiveness of combining advanced metaheuristic optimization with custom power devices to ensure the resilient, reliable, and sustainable operation of future EV–PV–dominated distribution networks.

**Keywords:** Photovoltaic distribution system, Electric vehicle charging, D-STATCOM, Dynamic control, Voltage stability, Enhanced Hunter–Prey Optimization (EHPO).

## 1. INTRODUCTION

### 1.1. Motivation for the work

The rapid adoption of renewable energy sources (PV, wind) and electric vehicles (EVs) is transforming distribution networks, introducing voltage fluctuations and power quality challenges due to their intermittent generation and variable demand [1]. EV charging further intensifies reactive power imbalances, risking grid instability. Effective reactive power management is therefore essential to ensure voltage stability, reduce losses, and enhance network efficiency. Traditional methods often fall short under such variable conditions, underscoring the need for adaptive, dynamic solutions that support voltage control and system flexibility [2]. This paper proposes a DSTATCOM-based dynamic-voltage-control strategy to mitigate the impacts of EV charging in PV-integrated distribution networks.

### 1.2. Literature

There is a growing need for reactive power control in electrical networks, particularly as decarbonization techniques are increasingly adopted [3]. Reactive power is closely connected to voltage and power quality, and its regulation plays a vital role in ensuring the desired system functioning. Articles [4-7] discuss the advantages of the smart grid, particularly its role in reducing system losses, voltage fluctuations, and operating costs, while also improving resilience, reliability, and power security. Volt/VAR control (VVC) has been a central research theme. Surveys in [8-10] provided overviews of the state of the art, focusing on smart distribution grids and on voltage regulation in low-voltage networks with high PV penetration. Building upon these reviews, coordinated multi-stage VVC strategies integrating Conservation Voltage Reduction (CVR), data-driven techniques, MPC-based VVC strategies and inverter-based distributed generation were proposed [11-14]. Articles [15-19] discuss the PV penetration in distribution systems, introducing local inverter-based VVC strategies with OPF-based coordinated active and reactive power controls. Hybrid voltage regulation methods that combine Q-compensating devices and PVs, along with intelligent rule-based designs for inverter-based Volt/VAR operations, have been tested on standard IEEE bus systems [20-22]. Further reconfiguration and use of optimization algorithms approach has been proposed in the works [23-25]. Table 1 below tabulates the literature discussed above.

**Table 1: Literature on various methodologies of VVC**

| Ref | Focus Area | Methodology/Approach | Key Contribution | Limitation / Gap |
|---|---|---|---|---|
| **[8]** | Network optimization under uncertainty | Review | Comprehensive survey on uncertainty methods | No implementation models |
| **[9]** | VVC in smart grids | Review | Taxonomy of VVC technologies | Lacks AI methods discussion |
| **[10]** | Voltage control in low voltage PV networks | Review | Summarizes PV-dominated network strategies | Focused only on PV |
| **[11]** | VVC with CVR and SOP | Multi-stage coordination | Hybrid CVR + inverter control | Complexity in large networks |
| **[12]** | Data-driven VVC | Data-driven optimization | Adaptive strategy without heavy models | Needs real-time validation |
| **[13]** | MPC-based VVC | MPC framework | Integrates CVR + DR via predictive model | Computationally heavy |
| **[14]** | Stochastic VVC + DR | Chance-constrained OPF | Probabilistic co-optimization | Uncertainty forecasting limited |
| **[17]** | Rule design for inverter DERs | Learning-based optimization | AI-designed Volt/VAR rules | Still simulation-based |
| **[19]** | OPF-based reactive/active power control | OPF optimization | Mitigation of voltage violation | Data requirement heavy |
| **[20]** | Smart inverter allocation | Optimal placement | Improves inverter impact | Site-specific validation lacking |
| **[21]** | PV allocation with AVR | Optimization | PV placement with AVR-based VVC | Does not integrate EVs |
| **[20]** | Coordinated VVC with OLTC+PV | State coordinated | Hybrid traditional-modern control | Does not consider uncertainty |
| **[22]** | Network reconfig + VVC | Mixed-integer optimization | Coordination in unbalanced systems | Early-stage methods |
| **[23]** | VAR + capacitor placement | Optimization in expandable grids | Reduces losses and costs | Limited stochastic handling |
| **[24]** | Network reconfig + renewables + capacitors under uncertainty | Stochastic optimization | Captures variability effects | Heavy computation |
| **[25]** | Reconfig + SOP multi-objective | Multi-objective OPF | Early formulation combining SOP + reconfig | Simplified assumptions |
| **[27]** | SOP optimization for PV + EV | Artificial Rabbits Optimization | Handles variable PV + EV | Metaheuristic efficiency issues |

The following literature review discusses conventional VVC devices, the negative impact on distribution networks resulting from EVCS and DG integration, and the need for advanced and dynamic solutions.

Studies [31-33] address the challenges of charging and discharging planning for EVs, as well as the sudden load fluctuations associated with the unpredictability of renewable energy. [34] highlights the over-EV and PV positioning challenges, stating that voltage dips, feeder losses, and thermal overloading are impacts of uncoordinated EV charging, and that voltage rise and rapid fluctuations are due to PV intermittency. These challenges exceed the capabilities of conventional devices, necessitating advanced, dynamic solutions.

Conventional methods of reactive power management have traditionally relied on on-load tap changers (OLTCs), voltage regulators (VRs), and capacitor banks (CBs). These devices are inexpensive and effective for steady-state regulation and Conservation Voltage Reduction (CVR) strategies [35]. However, their slow response, discrete operating steps, and frequent mechanical wear limit their effectiveness under fast-changing load and generation conditions [36].

Recent studies have explored a variety of modern control methods:

- Network Reconfiguration and CVR: Adaptive reconfiguration and CVR strategies have been used to minimize losses and peak demand. However, indices such as slower timescales and dependence on accurate models limit their effectiveness [22-24].
- PV Smart Inverters: PV inverters with Volt-VAR capabilities are used for localized reactive power support, like in the article [37]. However, their VAr capacity depends on real power output, making them unreliable during peak generation or low irradiance conditions.
- Energy Storage Systems (ESS): Battery storage integrated with inverters provides active and reactive flexibility, but high capital cost and state-of-charge constraints limit widespread adoption [28].

- Demand Response (DR) and EV Coordination: Shifting or rescheduling EV charging demand can reduce stress, but requires customer participation and a robust communication infrastructure, and is often too slow for sub-second voltage disturbances [38].
- Artificial Intelligence (AI) in Power Systems: Solar irradiance forecasting using the AI methods like the autoregressive moving average (ARMA) model and Random Forest [39,40]

Among the modern technologies mentioned above, Distribution Static Compensators (D-STATCOMs) stand out for their ability to provide fast, continuous, and smooth VAr injection. Unlike capacitor banks, D-STATCOMs respond within milliseconds, operate effectively and dynamically under low-voltage conditions, and can mitigate both under- and over-voltage [41]. According to [42, 43], they also enhance voltage stability, reduce losses, and address power quality issues within the integrated network. Optimal allocation and control of D-STATCOMs have been widely studied in the articles [44-46] using methods such as the student psychology-based optimization (SPBO) algorithm, Dwarf Mongoose Optimization (DMO), the flower pollination algorithm along with DG placement. The authors of [47] propose HPO for optimal DSTATCOM, PV and EVCS. Table 2 below gives the evolution of reactive power management techniques from OLTCs to DSTATCOMs.

**Table 2: Literature on the evolution of Reactive Power Management techniques**

| Ref | Method | Advantages | Limitations | Suitability under PV + EV stress |
|---|---|---|---|---|
| **[17-19,22]** | OLTCs and Voltage Regulators | Mature, widely deployed, low-cost | Slow response, mechanical wear, discrete steps | Limited |
| **[23,24]** | Capacitor Banks (CBs) | Cost-effective, simple installation | Fixed/stepwise VAr support, ineffective for fast fluctuations | Limited |
| **[24,25,35]** | CVR and Reconfiguration | Reduces losses and demand | Model-dependent, slower timescales | Moderate |
| **[37]** | PV Smart Inverters | Localized, fast response, supports grid codes | Limited by active power availability, coordination issues | Moderate |
| **[28]** | Energy Storage Systems (ESS) | Dual P/Q support, flexibility | High cost, SoC and lifetime constraints | High (but costly) |
| **[38]** | Demand Response and EV Control | Reduces peaks, shifts demand | Requires customer participation, slow response | Moderate |
| **[44-46]** | **D-STATCOMs** | Fast, continuous VAr injection, improves stability, dynamic response | Higher cost than CBs, needs optimal siting | Highly suitable |

The present study employs an Enhanced Hunter–Prey Optimization (EHPO) algorithm for optimal D-STATCOM allocation in IEEE 33, 69 and 118 bus systems, considering realistic PV and EV dynamic scenarios.

The contributions of the paper are:

- To determine the optimal locations of three units of PV, EVCS, and DSTATCOM using the proposed HPO for minimum active power losses.
- Fixing the optimal sizes and sites of PV and EVCS, and sites of DSTATCOM, the dynamic behaviour of DSTATCOM is analyzed using EHPO for the dynamic behaviour of PV and EV for four seasons (varying across 96 hours).
- Evaluating the dynamic DSTATCOM behaviour for its varying capacity on IEEE-33,69 and 118 bus systems.

Traditional metaheuristic methods like PSO and GA, and methods from literature such as [11], [14], although widely used, are known to suffer from premature convergence and limited exploration when applied to large-scale systems such as the IEEE-118 bus system. Hence, to offer a balanced exploration–exploitation mechanism inspired by predator–prey dynamics, HPO is preferred; to further improve convergence robustness by adding adaptive parameter control and a Cauchy mutation mechanism, the enhanced version (EHPO) is proposed in this work. The rest of the paper is sectionalized as follows: 2. Modelling concepts of the components, 3. Problem formulation, 4. Solution Methodology, 5. Results and Discussions, and 6. Conclusion.

## 2. MODELING OF CONCEPTS

### 2.1. Photovoltaic Systems

The active power of the PV is given by (1) below,

$$P_{PV} = P_{PVbase}\left[1 + \alpha_{PV} * \left(T - T_{ref}\right)\right] * \frac{SPV}{1000} \quad (1)$$

$P_{PV}$ is the active power output; $P_{PVbase}$ refers to the rated active power; 'αPV' is the temperature conversion coefficient; sPV is the solar irradiation; T and Tref are the current and reference temperature values, as the PV output depends on irradiance and temperature factors [48].

### 2.2. Electric Vehicle Charging Stations

In this study, Electric Vehicle Charging Stations are modelled as aggregated charging loads connected to the distribution network. Accordingly, at any node, m, the EV charging demand, $P_{EV}$ is added to the existing base load demand, resulting in the net active power demand at that node (Pm,net)

$$P_{m,net} = P_m + P_{EV,m} \quad (2)$$

The EV load demand can be modelled using a normal distribution, as described below.

The fluctuating and uncertain nature of the load can be estimated through probabilistic analysis. [50] uses the normal distribution function to define the load demand function using mean(μ) and standard deviation (σ), and is given in (3)

$$P_l = \frac{1}{\sqrt{2\pi}\times\sigma} e^{-\frac{(P_l-\mu^2)^2}{2\times\sigma^2}} \quad (3)$$

$P_l$ is the load demand.

### 2.3. D-STATCOM

The DSTATCOM custom power device is considered for the study. DSTATCOM integration offers advantages such as reduced active power losses, improved voltage stability, and improved power factor correction. The reactive power from D-STATCOM is modelled by [51],

$$Q_D = -|V_D|^2 B_D + |V_D|\left|V_g\right|B_D \quad (4)$$

Here, $Q_D$ is the D-STATCOM reactive power in kVAr, $|V_D|$ and $|Vg|$ are the D-STATCOM voltage and grid-bus voltages, respectively, with the susceptance of the D-STATCOM, $B_D$

When $|Vg| > |VD|$, for which $Q_D$ becomes negative and thus supplies the reactive power. Conversely, it absorbs reactive power from the grid if $|Vg| < |V_D|$, when $Q_D$ becomes positive.

At bus m, where the DSTATCOM is supposed to be placed, the net reactive power is estimated by (5)

$$Q_{net} = Q_m - Q_D \quad (5)$$

$Q_{net}$ denotes the net reactive power at the node m, with reactive power $Q_m$, and $Q_D$ is the reactive power from DSTATCOM.

### 2.4. Dynamic Net Loading Conditions

The authors of [52] demonstrated dynamic PV-EV conditions under sunny and cloudy weather, with PV generation coinciding with uncertain EV fleet charging. Work [53] illustrates that optimal day-ahead scheduling can balance charging costs and renewable utilization analyzing EV charging strategies under sunny and cloudy renewable generation scenarios. From equation (1), $s_{PV}$ is the solar irradiation, which is 0.9-1.0 for high sunny days producing stable to high PV output.

For $P_{EV\ rated}$ charging power of EV (kW), N is the number of EVs charging, u(t) being the charging probability (0-1), the aggregate EV charging can be given by (6) .

$$P_{EV(j)}(t) = N_{EV(j)}(t) * P_{EV} * u(t) \quad (6)$$

The number of EVs charging at node 'j', at time 't'. The uncertain EV load can be estimated by the binomial distribution function B from (7).

$$N_{EV(j)} \sim B(N_{tot,j}, p(t)) \quad (7)$$

$N_{tot,j}$ total number of EVs charging at the charging station at node 'j', and p(t) is the probability function, usually high at peak hours and low at base hours.

The effective net load at any k at instant t, can be given by (8),

$$P_{net,k}(t) = P_{l,k}(t) + P_{EV,k}(t) - P_{PV,k}(t) \quad (8)$$

$P_{net}$ is the effective load, $P_{EV}$ is the aggregate EV load, and $P_{PV}$ is the solar generation.

Four scenarios—sunny with low EV demand, sunny with high EV demand, cloudy with high EV demand, and cloudy with low EV demand — are the ones that can be studied under dynamic PV-EV integration.

## 3. PROBLEM FORMULATION

### 3.1. Objective Function

The active power loss minimization is taken as the objective. For an N-bus system, the Ploss is evaluated using (9).

$$P_{loss} = \sum_{k=1}^{N} |I_k|^2 * r_k \tag{9}$$

Ploss is the active power loss calculated on an N-bus system, where 'k' represents an individual bus, 'I' is the current flowing in the respective branch, and 'r' is its resistance.

### 3.2. Constraints

The proposed objective function is subjected to certain voltage and power constraints.

*Voltage constraint:*

$$V_{min} \leq V_k \leq V_{max} \tag{10}$$

From the above equation (10), the voltage at any node 'k' should lie between the limits (0.95.1.05).

*Active and reactive power constraints:*

Equations (11) and (12) define the active and reactive power limits of the distribution system.

$$P_{generated} + P_{PV} \geq P_{loss} + P_{demand} + P_{EVCS} \tag{11}$$

$$Q_{generated} + Q_D \geq Q_{loss} + Q_{demand} \tag{12}$$

The reactive power of the DSTATCOM is bounded between its minimum and maximum capacities; similarly, the active power from the PV is set to be within its lower and upper generation limits.

$$P_{PV\ min} \leq P_{PV} \leq P_{PV\ max} \tag{13}$$

$$Q_{D\ min} \leq Q_D \leq Q_{D\ max} \tag{14}$$

The above equation (14) ensures that the D-STATCOM operates within acceptable limits. In the absence of such bounds, a purely loss-minimization objective would result in excessive reactive power injection, which is not a viable solution.

## 4. SOLUTION METHODOLOGY

### 4.1 Hunter–Prey Optimization

Hunter Prey Optimization (HPO) is a recently developed nature-inspired meta-heuristic optimization algorithm by Naurei et al in 2021 [54]. The algorithm draws inspiration from the hunting strategies of carnivores, the escape tactics of prey, and the dynamic interactions between them. Like every other algorithm, HPO involves initialization, exploration and exploitation phases. The hunter's position is defined in the equation below,

$$x_i(t+1) = x_i(t) + 0.5[\left(2CZP - x_i(t)\right) + 2(1-C)Z\mu_i - x_i(t)] \tag{15}$$

The above equation defines the hunter's position relative to the iterations, with C as the balance parameter between exploration and exploitation, and Z as the adaptive parameter. Equation (16) gives the prey's escape position,

$$x_i\{t+1) = T_g + CZcos(2\pi R_4) \times (T_g - x_i(t)) \tag{16}$$

$T_g$ is the global maximum of the exploration-phase cosine function, which defines the next position. R4 is a random vector between [-1,1].

The exploitation phase is defined by using a random vector R5 and a regulating parameter 'β'=0.1. For R5>β, it's the prey's escape and if R5< β, then it's the hunting equation.

$$x_i(t+1) = \begin{cases} x_i(t) + 0.5[2(1-C)Z\mu - x_i(t) + 2CZP](a) \\ T_g + CZ\cos(2\pi R_4) \times \left(T_g - x_i(t)\right)(b) \end{cases} \tag{17}$$

### 4.2 Enhanced Hunter–Prey Optimization

The standard HPO is further enhanced by adapting a few features to improve its robustness. The algorithm is further tuned for fast, fine-grained convergence, avoiding early convergence errors and keeping the problem away from local minima traps more effectively, thereby providing enhanced HPO. Different versions of EHPO are discussed in [55].

#### 4.2.1 Initialization Phase Enhancement

The first stage of optimization, the initialization phase, is updated using Stochastic Reverse Learning and Tent Chaotic Mapping [56,57].

$$X_{rand} = l + b - r.X \tag{18}$$

u and l are the upper and lower limits, r is an arbitrary value between 0 and 1, X ε [l,u], and the random stochastic reverse solution is given by $X_{rand}$.

Tent mapping for manageable randomness of variables to abstain from the unstable fixed points and small periodic trappings during iterations, with d dimensions and N search agents, and u=0.5 is (19), the updated initialization is given in (20),

$$y_{i+1}^{d} = \begin{cases} 2\left(y_i^d + rand(0,1) \times \frac{1}{N}\right), & 0 \le y_i^d < 0.5 \\ 2\left(1 - y_i^d + rand(0,1) \times \frac{1}{N}\right), & 0.5 \le y_i^d < 1 \end{cases} \tag{19}$$

$$x_i^d = l + (u - l) \times y_i^j \tag{20}$$

#### 4.2.2 Step Size Updating

The authors of [58] improved the step-size representation of Brownian motion by considering both higher and lower step sizes.

$$iter < \frac{1}{3} maxit \tag{21}$$

$$S = \overrightarrow{R_B} \otimes (E - \overrightarrow{R_B} \otimes x_{i.j}(t)) \tag{22}$$

$$x_{i.j}(t+1) = x_{i,j}(t) + P \cdot \overrightarrow{R_B} \otimes S \tag{23}$$

The above equations (21-23) represent Brownian motion with a higher-step-size update (vector RB), where P=0.5, E is the finest solution matrix, iter is the number of iterations, and maxit is the maximum number of iterations. For a lower step size, the equations considered are,

$$it > \frac{1}{3} maxit \tag{24}$$

$$S = \overrightarrow{R_L} \otimes (\overrightarrow{R_L} \otimes x_{i.j}(t) - E) \tag{25}$$

$$x_{i.j}(t+1) = E + P \cdot CF \otimes S \tag{26}$$

The optimum solution matrix E, is given as

$$E = \begin{bmatrix} Xb_{1,1}^t & \cdots & Xb_{1,d}^t \\ \vdots & \ddots & \vdots \\ Xb_{1,n}^t & \cdots & Xb_{n,d}^t \end{bmatrix} \tag{27}$$

For n search agents and d dimensions, $X_b$ is the best solution.

#### 4.2.3 Enhancing Exploration and Exploitation Phases

To boost convergence speed and provide good local and global balance, the authors of [56] introduced inertia weights to enhance exploration during the early phase.

$$\omega = \omega_t * \frac{\omega_{max}}{\omega_{min}}^{\frac{1}{\frac{1+c.t}{maxit}}} \tag{28}$$

Where ω is the weight function, t is the current iteration, c is the adjustment parameter, maxit is the maximum number of iterations, and the maximum and minimum values are the weight adjustment parameters. The prey's escape or exploration phase (16) is updated as equation (29).

$$x_i(t+1) = \omega \times T_g + CZcos(2\pi R_4) \times (T_g - x_i(t)) \tag{29}$$

[57] adapts ESCA to improve the exploration and exploitation phases by Cauchy's mutation strategy.

***ESCA Adaptation:***

The finer global search capability of the SCA is applied to the standard HPO, considering,

$$P_v = \exp\left(\mu \times \left(\frac{t}{T}\right)^3\right) \tag{30}$$

$P_v$ gives the population position, with t being the current iteration number and T the maximum number of iterations. μ is the conversion factor. For any rand < $P_v$, the population position is updated using the ESCA, which is enhanced from SCA using hyperbolic sine controlling parameter; if rand > $P_v$, the position is updated using HPO. μ=0.01 by [59], and in [57], μ=-10.

***Cauchy's Strategy:***

Cauchy's mutation strategy is introduced to increase convergence speed and accuracy while avoiding local maxima trapping. The updated population is given as,

$$x_i^d(t+1) = r_1 \otimes x_i^d(t) + Cauchy \otimes (x_{best}^d(t) - x_i^d(t)) \quad (31)$$

$x_i^d(t)$ is the present position, $x_i^d(t+1)$ is the position after Cauchy mutation, $r_1$ is a random value ranging in [0,1]. The Cauchy mutation also avoids premature optimization.

**Table 3: Performance differences between the basic HPO and EHPO**

| Stage / Feature | Hunter–Prey Optimization (HPO) | Enhanced HPO (EHPO) | Improvement Achieved |
|---|---|---|---|
| **Initialization** | Random uniform population initialization | Tent chaotic mapping | Better exploration, avoids poor starting points |
| **Exploration Phase (Hunter Search)** | Prey locations updated using random step sizes | Adaptive step size (dynamic reduction with iteration) | Balances exploration and exploitation dynamically |
| **Exploitation Phase (Prey Escape)** | Fixed step movement towards the best solution | Mutation and Brownian motion inspired updates | Avoids premature convergence, increases diversity |
| **Escape Mechanism** | Randomized local movement | Hybrid local search with adaptive probability | Enhances fine-tuning of best solutions |
| **Parameter Control** | Fixed control parameters | Adaptive parameter tuning based on convergence rate | Improves convergence speed and robustness |
| **Optimization Efficiency** | Good at global search, but risk of stagnation near local optima | Robust search, prevents stagnation, and higher-quality final solutions | Higher accuracy and stability |
| **Application to D-STATCOM Control** | Provides optimal placement/sizing under static conditions | Provides **dynamic real-time tuning** of D-STATCOM under PV–EV variability | Enables continuous voltage/reactive power stability |
| **Convergence Profile** | Slower convergence, sometimes oscillatory | Faster and smoother convergence curves | Reduced computation time for real-time applications |

From Table 3 above, the Enhanced HPO (EHPO) addresses the limitations of the standard HPO by integrating chaotic initialization, adaptive parameter control, and hybrid local search strategies to improve convergence speed, solution diversity, and robustness, making EHPO particularly suited for real-time D-STATCOM control in PV–EV integrated distribution systems where fast and adaptive decision-making is critical.

### 4.3 Application of EHPO for Solving the Dynamic D-STATCOM Controls

The paper surveys the standard IEEE 33,69, and 118 systems with PV-EV variabilities for dynamic DSTATCOM control using the EHPO.

A dataset representing four days from four different seasons is considered. 96 hours (4*24) of PV, EV and load variations are contemplated. The dataset can be analyzed as follows in the Table 4.

## 5. RESULTS AND DISCUSSIONS

The simulations are analyzed in three different cases: comparison between the HPO and the EHPO algorithms, active power loss and voltage profile analysis using EHPO, and performance of DSTATCOM units in all three bus systems.

### 5.1. Case 1: Comparison between HPO and EHPO

To avoid early convergence and local minima traps, and to improve the robustness of the basic HPO, enhanced HPO (EHPO) is proposed. The proposed algorithm is studied on IEEE-33, 69, and 118 test bus systems for simultaneous placement of three units of each PV, EVCS, and DSTATCOM. The system performance is analyzed for active power losses reduction and voltage improvement, and the observations are recorded in Tables 5-7.

**Table 4: Table showing the EV-PV-Load variations across 96 hours**

| Scenario | Time Period (Hours) | PV Output(p.u.) | EV Demand(p.u.) | Base Load(p.u.) | Net Load Condition | Inference / D-STATCOM Need |
|---|---|---|---|---|---|---|
| **Sunny + Low EV demand (Daytime)** | Midday: 8–14, 32–38, 56–62, 80–86 | 0.7 - 0.9 | <0.05 | 0.82 - 1.08 | Netload reduced; sometimes below base load | Possible reverse power flow; low stress on the network |
| **Sunny + Moderate EV demand (Afternoon)** | Late afternoon: 14–18, 38–42, 62–66, 86–90 | 0.3 - 0.6 | 0.02 - 0.06 | 0.85 - 1.05 | Net load balanced; PV offsets part of EV demand | Stable condition; low D-STATCOM support needed |
| **Cloudy + High EV demand (Evening/Night)** | 18–24, 42–48, 66–72, 90–96 | ≈ 0 | 0.1 – 0.17 | >0.95 | Worst-case net load stress | High D-STATCOM support is required for reactive power stability |
| **Cloudy + Low EV demand (Night/Early hours)** | 1–6, 25–30, 49–54, 73–78 | ≈ 0 | <0.01 | 0.82 - 0.86 | Lightly loaded network | Minimal D-STATCOM support; network stable |

Figure 1 below gives the flowchart for the proposed EHPO algorithm.

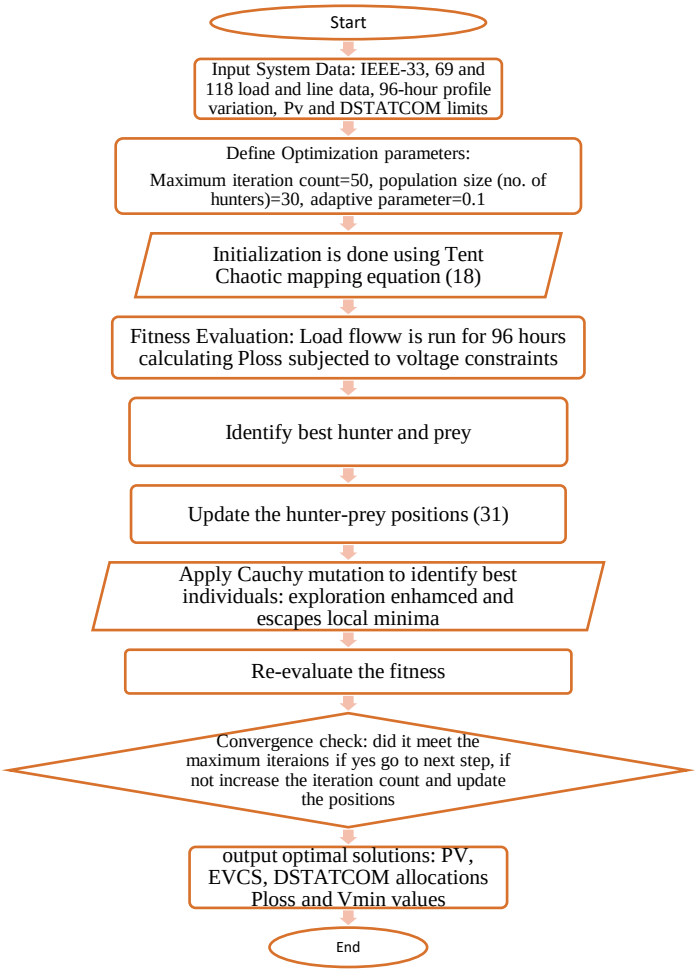


**Figure 1: Flow chart of the proposed EHPO algorithm**

The voltage profiles are improved using the EHPO in IEEE-33 and 118 systems and are nearly identical for the IEEE-69 bus system. The minimum voltage on the IEEE-33 bus is increased from 0.98 p.u. by HPO to 0.989 p.u. by EHPO, a 0.9% increase. The voltage profile decreases by 0.3% on the IEEE-69 bus when using the EHPO for HPO. The IEEE-118 bus system resulted in a 1.2% increase in the minimum voltage, rising from 0.956 p.u. with HPO to 0.968 p.u. using EHPO. There is a decrease from 17.99 kW to 12.59 kW in an IEEE-33 bus system, constituting a 30% decrease within the algorithms. In the IEEE-69 bus system, the active loss within the algorithms increases from 7.61 kW to 20.97 kW; however, EHPO yields a 90.68% reduction in loss. This is attributed to the high R/X ratio of the 69-bus network, which makes it highly sensitive to fluctuations in PV and EV loads. In the IEEE-118 bus system, active loss of 415.109 kW using HPO was further reduced to 279.075 kW using EHPO.

**Table 5: HPO and EHPO comparison in the IEEE-33 bus system**

| IEEE-33Bus /Parameter | HPO [47] | EHPO |
|---|---|---|
| DSTATCOM_1 (kVAr/bus) | 500 (11) | 360 (11) |
| DSTATCOM_2 (kVAr/bus) | 500 (24) | 429 (24) |
| DSTATCOM_3 (kVAr/bus) | 959.24 (30) | 844 (30) |
| Total Capacity (kVAr) | 1959.24 | 1633 |
| Ploss(kW) (base) | 210.99 | 210.99 |
| Ploss (kW)(optimized) | 17.99 | 12.59 |
| Vmin (p.u.) (base) | 0.9038 | 0.9038 |
| Vmin (p.u.) (optimized) | 0.98 | 0.989 |

**Table 6: HPO and EHPO comparison in the IEEE-69 bus system**

| IEEE-69Bus /Parameter | HPO [47] | EHPO |
|---|---|---|
| DSTATCOM_1 (kVAr/bus) | 500 (12) | 468 (12) |
| DSTATCOM_2 (kVAr/bus) | 827.578(28) | 202 (28) |
| DSTATCOM_3 (kVAr/bus) | 1214.23 (61) | 1022 (61) |
| Total Capacity (kVAr) | 2541.808 | 1692 |
| Ploss (kW)(base) | 225.0 | 225.0 |
| Ploss (kW)(optimized) | 7.61 | 20.97 |
| Vmin (p.u.)(base) | 0.909 | 0.909 |
| Vmin (p.u.)(optimized) | 0.99 | 0.987 |

**Table 7: HPO and EHPO comparison in IEEE-118 bus system**

| IEEE-118 Bus /Parameter | HPO [47] | EHPO |
|---|---|---|
| DSTATCOM_1 (kVAr/bus) | 3714.6 (34) | 2700 (34) |
| DSTATCOM_2 (kVAr/bus) | 1000 (74) | 1000 (74) |
| DSTATCOM_3 (kVAr/bus) | 2344.60 (110) | 1956 (110) |
| Total Capacity (kVAr) | 7059.2 | 5656 |
| Ploss(kW)(base) | 1296.696 | 1296.696 |
| Ploss (kW)(optimized) | 415.109 | 279.075 |
| Vmin (p.u.) (base) | 0.869 | 0.869 |
| Vmin (p.u.) (optimized) | 0.956 | 0.968 |

From the above-mentioned tables, it can be observed that the DSTATCOM sizes for all three units at minimum losses are smaller than those for HPO using the EHPO. This accounts for the minimization of component cost reduction. The EHPO results in 16.64% reduction for the IEEE-33 bus system, 33.43% for the IEEE-69 bus system, and 19.87% for the IEEE-118 bus system.

### 5.2. Case 2: Power loss reduction and voltage profile analysis using EHPO

For an IEEE-33 bus system, when analyzed for driving DSTATCOM operation with PV-EV-load variations, the minimum active power loss is 12.59 kW, and the minimum voltage is 0.92 pu. Minimum loss is attained at the 15th hour with 360 kVAR, 429 kVAr, and 844 kVAr as DSTATCOM capacities, and corresponding voltage of 0.988 p.u.

In an IEEE-69 system using EHPO, minimum active power losses of 20.97 kW are observed at the 15th hour, with DSTATCOM ratings of 468 kVAr, 204 kVAr, and 1022 kVAr at that hour, and a minimum voltage of 0.9871 p.u. In the 118 system, the minimum loss is 279.075 kW at the 14th hour with a minimum voltage of 0.9682 pu. Table 10 presents the recorded DSTATCOM sizes corresponding to the minimum loss, namely 2740 kVAr, 1000 kVAr, and 1956 kVAr.

In addition to instantaneous performance indices, the average active power loss and minimum voltage are reported in Table 9 to reflect the overall system behaviour during the study period. Table 9 below presents the average active power loss and minimum voltage values for all three IEEE-33, 69, and 118 bus systems. The overall performance is estimated from average values; the

active loss reduction is 61.95%, 61.47%, and 51.15% in IEEE-33, 69, and 118 bus systems, respectively. And the minimum voltage averages to 0.952 p.u., 0.956 p.u., and 0.921 p.u., respectively.

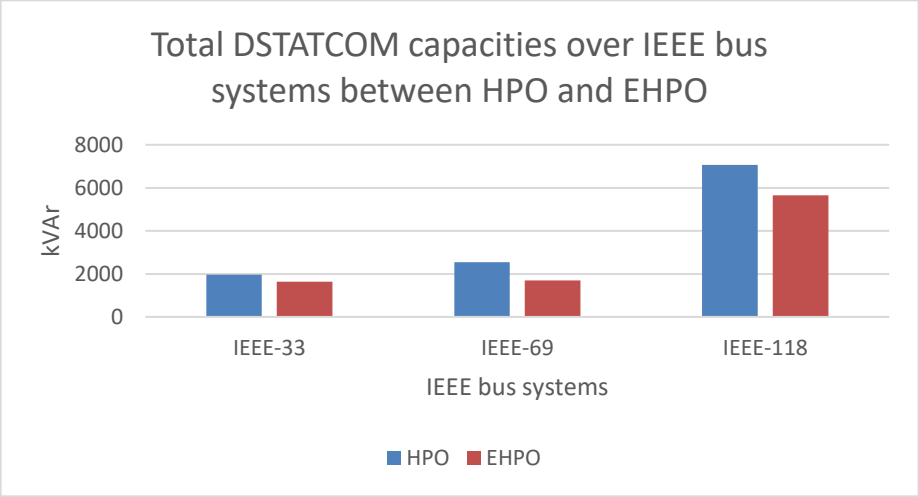


**Figure 2: DSTATCOM capacity comparison between the HPO and EHPO algorithms**

**Table 8: Performance analysis of three DSTATCOM units in IEEE-33, 69, and 118 bus systems using the EHPO**

| Bus system | Hour of minimum loss | DS1 (kVAr) | DS2 (kVAr) | DS3 (kVAr) | Ploss (kW) | Vmin (pu) |
|---|---|---|---|---|---|---|
| **33** | 15 | 360 | 429 | 844 | 12.59 | 0.988 |
| **69** | 15 | 468 | 204 | 1022 | 20.97 | 0.987 |
| **118** | 14 | 2700 | 1000 | 1956 | 279.075 | 0.968 |

**Table 9: Average actual loss and voltage minimum values over 96 hours for IEEE-33, 69, and 118 bus systems**

| Parameter | IEEE-33 | 69 | 118 |
|---|---|---|---|
| **Base case Ploss(kW)** | 210.99 | 225.30 | 1296.696 |
| **Average Ploss (kW)** | 80.28(61.95%) | 86.68(61.47%) | 633.4(51.15%) |
| **Average Voltage minimum (p.u.)** | 0.952 | 0.956 | 0.921 |

Figure 3 below illustrates the hourly variations in active power loss and minimum voltage for all three IEEE-33, 69, and 118 bus systems. From the figure, the voltage values are around 0.92 p.u. observed in Fig. 3(b), (d), and (f) correspond to short-duration peak loading conditions and represent instantaneous worst-case scenarios but not sustained operating points. In the uncompensated case, the minimum bus voltage records 0.9038 p.u. for the IEEE-33 bus system, 0.909 p.u. for the IEEE-69 bus system, and 0.867 p.u. for the IEEE-118 bus system, which, with the proposed EHPO algorithm, improves to 0.989 p.u., 0.987 p.u., and 0.968 p.u., respectively. And the algorithm limits the minimum voltage to approximately 0.92 p.u.,(0.88p.u. in the IEEE-118 system) even under peak loading and worst-operating scenarios with heavy demand, thereby demonstrating substantial voltage recovery. To achieve a strict lower limit of 0.95 p.u. in every case may require increased DSTATCOM capacities or additional compensating devices, which are currently not part of this study and could be included in the extended scope.

### 5.3. Case 3: DSTATCOM performance analysis

The performance of the three optimally sited DSTATCOMs on the IEEE-33 bus system was analyzed over 96 hours of varying PV generation, EV charging load, and overall system demand. Statistical metrics, including mean, median, standard deviation (SD), coefficient of variation (CV), and capacitor saturation, were calculated for each site.

Mean: The mean reactive power output of each DSTATCOM indicates the average size required over the 96-hour period to meet system demand.

Median: The median represents the central tendency and helps to understand typical operation, less affected by extreme hours.

Standard deviation (SD): The SD shows the variability in DSTATCOM size over 96 hours. A higher SD indicates greater fluctuation due to PV-EV-load changes.

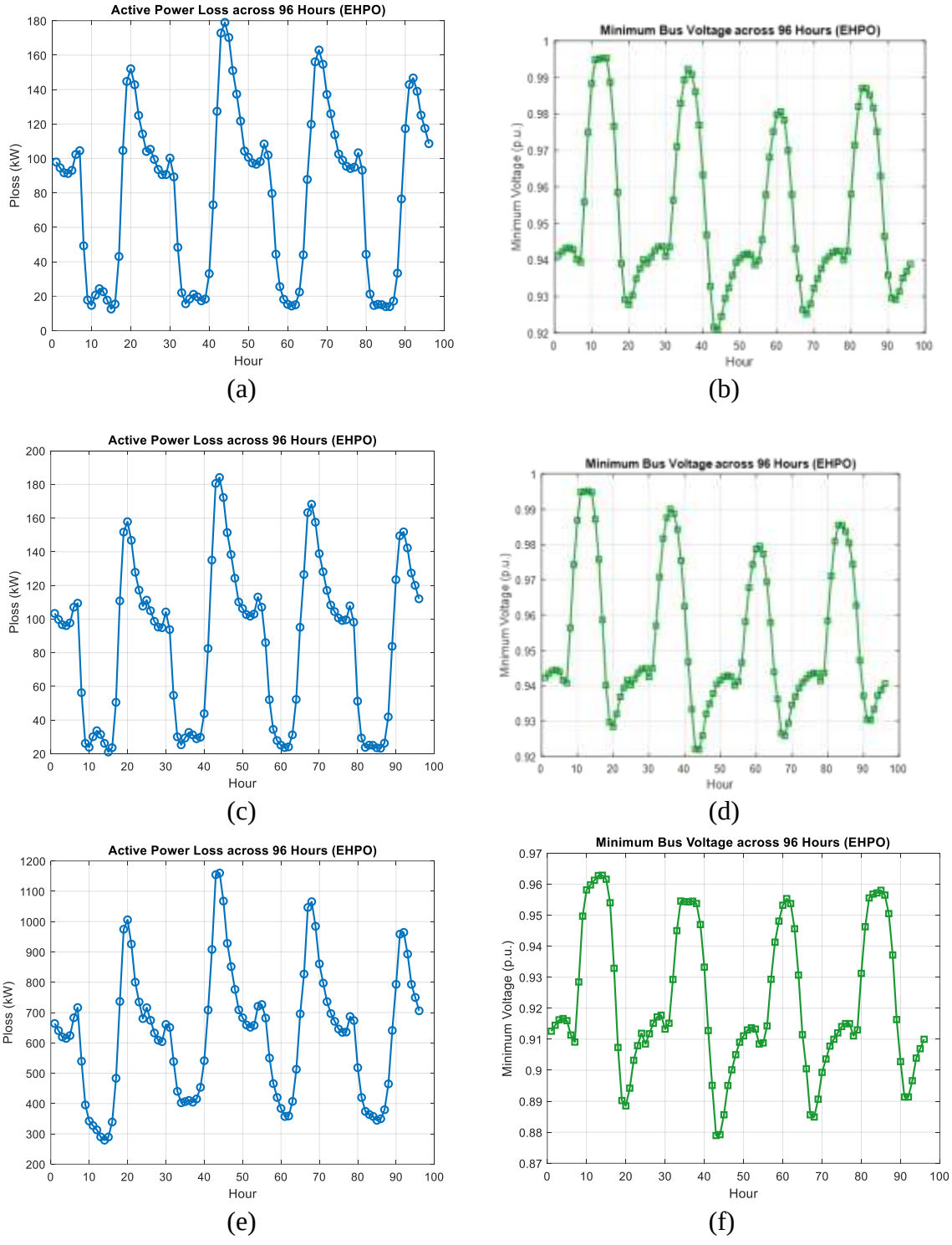


**Figure 3: (a,c,e) Active power loss variations in IEEE-33, 69, and 118 bus systems; (b,d,f) voltage variations in the respective systems**

Coefficient of Variation (CV): CV normalizes the SD relative to the mean, providing a dimensionless measure of variability. A low CV indicates that the system has predictable and stable compensation requirements. A high CV indicates that DSTATCOM requirements are inconsistent, and the network is at risk of instability and sizing challenges.

Capacity Saturation (%): Capacity saturation indicates the percentage of hours in which the DSTATCOM operated at its maximum rated capacity.

The performance indices of the three DSTATCOM units are tabulated in Table 5 below. DSTATCOM1 exhibited an average (mean) size of 407.48 kVAr with a median of 397 kVAr, a standard deviation of 36.94 kVAr, and a CV of 0.09, operating at its maximum rating (500 kVAr) for approximately 5.21% of the hours. DSTATCOM2 had a higher mean size of 471.32 kVAr, median 471.5 kVAr, SD of 23.48 kVAr, and CV of 0.05, with saturation occurring around 25% of the time. DSTATCOM3 showed the largest mean size of 907.28 kVAr, median 914.50 kVAr, SD of 45 kVAr, and CV of 0.05, reaching its rated limit of 960 kVAr for nearly 22.92% of the period.

These results indicate that while DSTATCOM1 and DSTATCOM2 provided sufficient reactive support under most conditions, DSTATCOM1 operated in its maximum limit of 500 kVAr for 5 hours in 96 hours. DSTATCOM2 operated at 500 kVAr for 24 hours, the maximum time among all three, while DSTATCOM3 was more heavily loaded during peak PV and EV scenarios, reaching 996 kVAr for 22 hours. The relatively low CV values suggest that, despite hourly variations in PV, EV, and load, the required reactive compensation remained stable, demonstrating the effectiveness of the EHPO-based sizing strategy. Overall, all three DSTATCOMs successfully supplied the necessary reactive power, with DSTATCOM3 approaching its maximum rating under extreme operating conditions and DSTATCOM2 operating at its maximum capacity most of the time. Similar results are observed for IEEE-69 and 118 systems. The respective parameters of the three DSTATCOMs are listed in the tables below.

**Table 10: Performance parameters of the three DSTATCOM units in IEEE-33 bus system**

| Site (bus) | Mean (kVAr) | Median (kVAr) | SD (kVAr) | CV | Max Rating (kVAr) | Saturation (%) |
|---|---|---|---|---|---|---|
| **11** | 407.48 | 397 | 36.94 | 0.09 | 500 | 5.21 |
| **24** | 471.32 | 471.5 | 23.48 | 0.05 | 500 | 25 |
| **30** | 907.28 | 914.5 | 45.00 | 0.05 | 960 | 22.92 |

**Table 11:Performance parameters of the three DSTATCOM units in IEEE-69 bus system**

| Site (bus) | Mean (kVAr) | Median (kVAr) | SD (kVAr) | CV | Max Rating (kVAr) | Saturation (%) |
|---|---|---|---|---|---|---|
| **12** | 491.92 | 500 | 12.80 | 0.02 | 500 | 60.4% |
| **28** | 248.53 | 348 | 64.90 | 0.26 | 391 | 1.04% |
| **61** | 1119.38 | 1119 | 67.10 | 0.06 | 1215 | 18.75% |

**Table 12: Performance parameters of the three DSTATCOM units in IEEE-118 bus system**

| Site (bus) | Mean (kVAr) | Median (kVAr) | SD (kVAr) | CV | Max Rating (kVAr) | Saturation (%) |
|---|---|---|---|---|---|---|
| **34** | 3021.13 | 2992 | 222.86 | 0.074 | 3463 | 1.04 |
| **74** | 1000 | 1000 | 0 | 0.0 | 1000 | 100 |
| **110** | 2122.72 | 2109 | 137.04 | 0.065 | 2345 | 9.37 |

From Table 12, it can be observed that for Site 74 in the IEEE-118 bus system, the D-STATCOM operates at 100% saturation with zero standard deviation over the 96-hour horizon, indicating continuous utilization of its rated capacity. This behaviour does not imply an optimization failure; rather, it highlights that the particular node is an electrically weak location under heavy loading conditions and is seeking sustained reactive power demand. Increasing the maximum reactive power capacity would further alleviate saturation and improve voltage regulation, but it would also result in higher capital investment. Therefore, the observed saturation reflects a constrained yet technically optimal solution within the considered capacity limits.

A supplementary sensitivity study with an increased reactive power upper limit for the second DSTATCOM revealed that the active power losses profile remains nearly unchanged, with a minimum of 279.1 kW. The D-STATCOM operates with time-varying reactive dispatch rather than continuous saturation, and the worst-case minimum voltage improved from 0.88 p.u. to 0.89 p.u. This confirms that the originally selected bounds ensure loss-optimality, whereas increased limits primarily enhance voltage security.

## 6. CONCLUSION

This study presented a dynamic control strategy for D-STATCOM allocation in PV- EV integrated distribution systems using an Enhanced Hunter–Prey Optimization (EHPO) algorithm. The proposed method was validated on the IEEE 33, 69, and 118-bus test systems under 96-hour operational scenarios. Key conclusions are as follows:

- EHPO-based allocation of D-STATCOMs significantly reduced active power loss and enhanced voltage stability compared to uncompensated cases and conventional HPO.
- Dynamic control was particularly beneficial in mitigating voltage dips during peak EV charging and in accommodating PV intermittency.
- The approach demonstrated scalability, with notable improvements in larger systems such as the IEEE 118-bus network.

**Table 13: Overall performance analysis between HPO and EHPO in IEEE-33,69, & 118 bus systems**

| Test System | HPO (Static Case) | EHPO (Dynamic Case) | Observed Outcome | Justification |
|---|---|---|---|---|
| **IEEE-33** | Optimal placements under fixed load/PV/EV scenario; achieves good loss reduction. | DSTATCOM operates under varying PV–EV–load curves with adaptive EHPO. | **Loss reduction and voltage enhancement are better than HPO.** | In smaller systems, dynamic variations expose HPO's limitation of being tuned to one condition. EHPO adapts and tracks dynamic changes, improving loss and voltage profiles. |
| **IEEE-69** | Placements tuned to a static condition; achieves the **lowest losses** under a fixed scenario. | Dynamic PV–EV variations applied; EHPO prioritizes stability across all conditions. | **Slightly higher loss than HPO. The voltage profile is almost maintained the same** | A mid-sized system with a high R/X ratio is sensitive to fluctuations. Static HPO placements do not remain optimal over time. EHPO is subject to a slight increase in pure loss minimization to maintain dynamic voltage stability. |
| **IEEE-118** | High-dimensional search; HPO risks premature convergence under the static case. Yielded good loss reduction | Dynamic EHPO effectively manages large-scale variations in PV–EV systems. | **Loss reduction and the voltage profile were better than with HPO.** | In large systems, EHPO's enhanced exploration avoids poor local minima and dynamically optimizes, outperforming static HPO in both loss reduction and voltage profiles. |

Future work will focus on extending the proposed methodology to include coordinated operation of multiple custom power devices (PV-ESS-DSTATCOM), real-time control strategies under stochastic PV and EV conditions, and validation on practical distribution feeders.

**Acknowledgments**

The authors thank the Department of Electrical Engineering, Christ University, and further declare that they received no specific funding for this work.

**Authors' Contributions**

In this study, the first author contributed towards the modelling, simulation experiments, and manuscript drafting. The second author contributed to conceptualization, methodological development, optimization algorithm design and implementation. Both authors participated in manuscript revision and approved the final submission.

**Competing Interests**

The authors declare that they have no conflict of interest.

**References**

[1] Pathak, A. K., M. P. Sharma, and Mahesh Bundele. "A critical review of voltage and reactive power management of wind farms." Renewable and Sustainable Energy Reviews 51 (2015): 460-471. https://doi.org/10.1016/j.rser.2015.06.015

[2] Hofmann, Wolfgang, Jürgen Schlabbach, and Wolfgang Just. Reactive power compensation: a practical guide. John Wiley & Sons, 2012.

[3] Potter, Adam, et al. "A reactive power market for the future grid." Advances in Applied Energy 9 (2023): 100114. https://doi.org/10.1016/j.adapen.2022.100114

[4] F. Li, W. Qiao, H. Sun, H. Wan, J. Wang, Y. Xia, et al., "Smart transmission grid: Vision and framework", IEEE Trans. Smart Grid, vol. 1, no. 2, pp. 168-177, Sep. 2010.

[5] R. Sirjani and A. R. Jordehi, "Optimal placement and sizing of distribution static compensator (D-STATCOM) in electric distribution networks: A review", Renew. Sustain. Energy Rev., vol. 77, pp. 688-694, Sep. 2017.

[6] M. Madrigal, R. Uluski and K. M. Gaba, "The concept role and priorities of smart grids" in Practical Guidance for Defining a Smart Grid Modernization Strategy, Washington, DC, USA:World Bank Group, pp. 1-14, 2017.

[7] K. Moslehi and R. Kumar, "A reliability perspective of the smart grid", IEEE Trans. Smart Grid, vol. 1, no. 1, pp. 57-64, May 2010.

[8] Liao H. Review on distribution network optimization under uncertainty. Energies. 2019 Sep 1;12(17):3369.

[9] Gholami K, Islam MR, Rahman MM, Azizivahed A, Fekih A. State-of-the-art technologies for volt-var control to support the penetration of renewable energy into the smart distribution grids. Energy Reports. 2022 Nov 1;8:8630-51.

[10] Gao X, Zhang J, Sun H, Liang Y, Wei L, Yan C, Xie Y. A review of voltage control studies on low voltage distribution networks containing high penetration distributed photovoltaics. Energies. 2024 Jun 21;17(13):3058.

[11] Pamshetti VB, Singh S, Thakur AK, Singh SP. Multistage coordination Volt/VAR control with CVR in active distribution network in presence of inverter-based DG units and soft open points. IEEE Transactions on Industry Applications. 2021 Mar 3;57(3):2035-47.
[12] Sun X, Qiu J, Tao Y, Ma Y, Zhao J. A multi-mode data-driven volt/var control strategy with conservation voltage reduction in active distribution networks. IEEE Transactions on Sustainable Energy. 2022 Feb 8;13(2):1073-85.
[13] Dutta A, Ganguly S, Kumar C. MPC-based coordinated voltage control in active distribution networks incorporating CVR and DR. IEEE Transactions on Industry Applications. 2022 Mar 29;58(4):4309-18.
[14] Najafi S, Livani H, Benidris M. Chance constraint co-optimization of volt/var and demand response in distribution networks. In2023 IEEE Power & Energy Society General Meeting (PESGM) 2023 Jul 16 (pp. 1-5). IEEE.
[15] Shaheen AM, Elattar EE, Nagem NA, Nasef AF. Allocation of PV systems with Volt/Var control based on automatic voltage regulators in active distribution networks. Sustainability. 2023 Nov 5;15(21):15634.
[16] Chen M, Ma S, Soltani Z, Ayyanar R, Vittal V, Khorsand M. Optimal placement of pv smart inverters with volt-var control in electric distribution systems. IEEE Systems Journal. 2023 Apr 10;17(3):3436-46.
[17] Murzakhanov I, Gupta S, Chatzivasileiadis S, Kekatos V. Optimal design of Volt/VAR control rules for inverter-interfaced distributed energy resources. IEEE Transactions on Smart Grid. 2023 May 25;15(1):312-23.
[18] Sun X, Qiu J, Zhao J. Optimal local volt/var control for photovoltaic inverters in active distribution networks. IEEE Transactions on Power systems. 2021 May 13;36(6):5756-66.
[19] Wagle R, Sharma P, Sharma C, Amin M. Optimal power flow based coordinated reactive and active power control to mitigate voltage violations in smart inverter enriched distribution network. International Journal of Green Energy. 2024 Jan 26;21(2):359-75
[20] Singh PP, Palu I. State coordinated voltage control in an active distribution network with on-load tap changers and photovoltaic systems. Global Energy Interconnection. 2021 Apr 1;4(2):117-25.
[21] Shaheen AM, Elattar EE, Nagem NA, Nasef AF. Allocation of PV systems with Volt/Var control based on automatic voltage regulators in active distribution networks. Sustainability. 2023 Nov 5;15(21):15634.
[22] Liu Y, Li J, Wu L. Coordinated optimal network reconfiguration and voltage regulator/DER control for unbalanced distribution systems. IEEE Transactions on Smart Grid. 2018 Mar 15;10(3):2912-22.
[23] Mahdavi M, Alshammari NF, Awaafo A, Jurado F, Gopi P. An economic loss reduction using static VAR compensator and capacitor placement in reconfigurable and expandable distribution grids with a variable electric power demand. IEEE Transactions on Industry Applications. 2025 Feb 24.
[24] Sayed MM, Mahdy MY, Abdel Aleem SH, Youssef HK, Boghdady TA. Simultaneous distribution network reconfiguration and optimal allocation of renewable-based distributed generators and shunt capacitors under uncertain conditions. Energies. 2022 Mar 21;15(6):2299.
[25] Qi, Qi, et al. "Multi-objective optimization of electrical distribution network operation considering reconfiguration and soft open points." Energy Procedia 103 (2016): 141-146.
[26] Wang J, Wang WQ, Wang HY. Bi-stage operation optimization of active distribution networks with soft open point considering violation risk. Energy Reports. 2022 Nov 1;8:14947-61.
[27] Janamala V, Radha Rani K, Sobha Rani P, Venkateswarlu AN, Inkollu SR. Optimal switching operations of soft open points in active distribution network for handling variable penetration of photovoltaic and electric vehicles using artificial rabbits optimization. Process Integration and Optimization for Sustainability. 2023 Mar;7(1):419-37
[28] Sharma S, Niazi KR, Verma K, Rawat T. Impact of battery energy storage, controllable load and network reconfiguration on contemporary distribution network under uncertain environment. IET Generation, Transmission & Distribution. 2020 Nov;14(21):4719-27
[29] Rehman, Asad, et al. "Critical Issues of Optimal Reactive Power Compensation Based on an HVAC Transmission System for an Offshore Wind Farm." Sustainability 15.19 (2023): 14175. https://doi.org/10.3390/su151914175
[30] Guo, Wang, and Wu Xu. "Research on optimization strategy of harmonic suppression and reactive power compensation of photovoltaic multifunctional grid connected inverter." International Journal of Electrical Power & Energy Systems 145 (2023): 108649. https://doi.org/10.1016/j.ijepes.2022.108649
[31] Hou, Luyang, et al. "Energy management for solar-hydrogen microgrids with vehicle-to-grid and power-to-gas transactions." International Journal of Hydrogen Energy 48.5 (2023): 2013-2029. https://doi.org/10.1016/j.ijhydene.2022.09.238
[32] Abubakr, Hussein, et al. "Adaptive frequency regulation strategy in multi-area microgrids including renewable energy and electric vehicles supported by virtual inertia." International Journal of Electrical Power & Energy Systems 129 (2021): 106814. https://doi.org/10.1016/j.ijepes.2021.106814
[33] Zand, Mohammad, et al. "Energy management strategy for solid-state transformer-based solar charging station for electric vehicles in smart grids." IET renewable power generation 14.18 (2020): 3843-3852. https://doi.org/10.1049/iet-rpg.2020.0399
[34] Dubey, Anamika, and Surya Santoso. "Electric vehicle charging on residential distribution systems: Impacts and mitigations." IEEe Access 3 (2015): 1871-1893.
[35] Padullaparti, Harsha, et al. "Conservation voltage reduction with distributed energy resource management system, grid-edge, and legacy devices." 2023 IEEE Power & Energy Society General Meeting (PESGM). IEEE, 2023.
[36] Sirjani, Reza, and Ahmad Rezaee Jordehi. "Optimal placement and sizing of distribution static compensator (D-STATCOM) in electric distribution networks: A review." Renewable and Sustainable Energy Reviews 77 (2017): 688-694.
[37] Zhao, Xin, et al. "Power system support functions provided by smart inverters—A review." CPSS Transactions on Power Electronics and Applications 3.1 (2018): 25-35.
[38] Bhattarai, Bishnu P., et al. "Design and cosimulation of hierarchical architecture for demand response control and coordination." IEEE Transactions on Industrial Informatics 13.4 (2016): 1806-1816.
[39] H. Cheng, W.-S. Cao, and P.-J. Ge, “Forecasting research of long-term solar irradiance and output power for photovoltaic generation system,” in Proc. 4th Int. Conf. Comput. Inf. Sci., Aug. 2012, pp. 1224–1227
[40] Nallakaruppan, M. K., et al. "Advancing solar energy integration: Unveiling XAI insights for enhanced power system management and sustainable future." Ain Shams Engineering Journal 15.6 (2024): 102740.
[41] Adepoju, Gafari Abiola, et al. "Impact of DSTATCOM penetration level on technical benefits in radial distribution network." e-Prime-Advances in Electrical Engineering, Electronics and Energy 7 (2024): 100413.
[42] Gupta, Atma Ram, and Ashwani Kumar. "Impact of DG and D-STATCOM placement on improving the reactive loading capability of mesh distribution system." Procedia Technology 25 (2016): 676-683.
[43] Gholami, Khalil, et al. "State-of-the-art technologies for volt-var control to support the penetration of renewable energy into the smart distribution grids." Energy Reports 8 (2022): 8630-8651.
[44] Dash, Subrat Kumar, et al. "Optimal planning of multitype DGs and D-STATCOMs in power distribution network using an efficient parameter free metaheuristic algorithm." Energies 15.9 (2022): 3433.
[45] Raj, A. Ferminus, and A. Gnana Saravanan. "An optimization approach for optimal location & size of DSTATCOM and DG." Applied Energy 336 (2023): 120797.
[46] Ganesh, Selvaraj, and Rajangam Kanimozhi. "Meta-heuristic technique for network reconfiguration in distribution system with photovoltaic and D-STATCOM." IET Generation, Transmission & Distribution 12.20 (2018): 4524-4535.

[47] Pappu, Soundarya Lahari, Varaprasad Janamala, and A. S. Veerendra. "Hunter–Prey Optimization Algorithm for Optimal Allocation of PV, DSTATCOM, and EVCS in Radial Distribution Systems." Advanced Control for Applications: Engineering and Industrial Systems 6.4 (2024): e231.
[48] Brini, Saoussen, Hsan Hadj Abdallah, and Abderrazak Ouali. "Economic dispatch for power system included wind and solar thermal energy." Leonardo Journal of Sciences 14.2009 (2009): 204-220.
[49] Huang, Liping, et al. "Electric Vehicle Cluster Scheduling Model for Distribution Systems Considering Reactive-Power Compensation of Charging Piles." Energies 17.11 (2024): 2541
[50] Gholami, Khalil, et al. "Voltage stability improvement of distribution networks using reactive power capability of electric vehicle charging stations." Computers and Electrical Engineering 116 (2024): 109160. https://doi.org/10.1016/j.compeleceng.2024.109160
[51] Giridhar, M. S., et al. "Mayfly Algorithm for Optimal Integration of Hybrid Photovoltaic/Battery Energy Storage/D-STATCOM System for Islanding Operation." International Journal of Intelligent Engineering & Systems 15.3 (2022).
[52] Pandraju, T. K. S., & Janamala, V. (2021). Dynamic optimal network reconfiguration under photovoltaic generation and electric vehicle fleet load variability using self-adaptive butterfly optimization algorithm. Int. J. Emerging Electric Power Systems. https://doi.org/10.1515/ijeeps-2021-0009
[53] Şengör, İbrahim, et al. "Day-ahead charging operation of electric vehicles with on-site renewable energy resources in a mixed integer linear programming framework." IET smart grid 3.3 (2020): 367-375.
[54] Naruei, Iraj, Farshid Keynia, and Amir Sabbagh Molahosseini. "Hunter–prey optimization: Algorithm and applications." Soft Computing 26.3 (2022): 1279-1314.
[55] Lahari, Pappu Soundarya, and Varaprasad Janamala. "Hunter–Prey Optimization Algorithm: a review." Journal of Electrical Systems and Information Technology 11.1 (2024): 19.
[56] Wang, Xiangyue, et al. "Short-term wind power prediction by an extreme learning machine based on an improved hunter–prey optimization algorithm." sustainability 15.2 (2023): 991
[57] Fu, Mingxin, and Qiang Liu. "An Improved Hunter-prey Optimization Algorithm and Its Application." 2022 IEEE International Conference on Networking, Sensing and Control (ICNSC). IEEE, 2022
[58] Hassan, Mohamed H., et al. "An enhanced hunter-prey optimization for optimal power flow with FACTS devices and wind power integration." IET Generation, Transmission & Distribution (2023).
[59] He Qing, Xu Qinshuai, Wei Kangyuan. Optimization of wireless sensor node deployment based on improved sine cosine algorithm [J]. Computer Application, 2019, 39 (07): 2035-2043
[60] Singh, Mukesh, Praveen Kumar, and Indrani Kar. "Implementation of vehicle to grid infrastructure using fuzzy logic controller." IEEE Transactions on Smart Grid 3.1 (2012): 565-577.